



A useful scaffold based on acenaphthene exhibiting Cu^{2+} induced excimer fluorescence and sensing cyanide via Cu^{2+} displacement approach

Mohammad Shahid, Syed S. Razi, Priyanka Srivastava, Rashid Ali, Biswajit Maiti, Arvind Misra*

Department of Chemistry, Faculty of Science, Banaras Hindu University, Varanasi 221 005, India

ARTICLE INFO

Article history:

Received 31 May 2012

Received in revised form 1 August 2012

Accepted 17 August 2012

Available online 24 August 2012

Keywords:

Chemosensor

Cu^{2+}

CN^-

Excimer

ABSTRACT

A new simple organic scaffold based on acenaphthene **4** was designed and synthesized. The chromogenic and fluorogenic properties of **4** toward different metal ions and anions were investigated in $\text{H}_2\text{O}/\text{MeCN}$ (8:2, v/v) solution. The probe **4** in the presence of Cu^{2+} exhibited strong static excimer emission at 507 nm along with a decrease in monomer emission at ~ 400 nm ratiometrically, attributed to a complexation through aldimine and amide groups of **4**. Additionally, **4** upon interaction with different anions illustrated significant fluorescence enhancement with cyanide. However, interaction of complex, **4**- Cu^{2+} with CN^- revealed fluorescence quenching attributed to formation of stable $[\text{Cu}(\text{CN})_x]^{1-x}$ species in the medium. A naked-eye sensitive fluorescent green color of solution was changed to blue. The mechanism of interaction between **4** and Cu^{2+} and sensing of cyanide through Cu^{2+} displacement approach was confirmed by the change in optical behaviors and ^1H NMR and ESI-MS spectral data analysis.

© 2012 Elsevier Ltd. All rights reserved.

1. Introduction

The development of selective and sensitive methods to detect cations and anions have received considerable attention because of important roles of these ions in biological, environmental, and industrial processes.¹ Recently, major emphasis is on design and development of novel organic scaffolds that can be potentially utilized as a colorimetric and fluorescent sensors for cations and anions and allow the sensing event, sensitive to naked-eye detection by a color change, and without resorting expensive and sophisticated instruments.² Among the several approaches fluorescent based methods have advantages due to their high sensitivity, specificity, real time monitoring, and fast response time.³ Moreover, the ratiometric fluorescent sensors, which are sensitive to variation in relative emission intensity, upon binding with ions are preferred because the ratio of dual emission intensities can be utilized to analyze the analyte concentration and to provide a built-in correction for effects, such as, photobleaching, sensor molecule concentration, the environment around the sensor molecules (pH, polarity, temperature, and so forth) and stability on photoirradiation.⁴

Among the soft transition metal ions and anions copper play important role in various biological processes, such as, a catalytic cofactor of a variety of metalloenzymes for instance superoxide dismutase, cytochrome-c oxidase, and tyrosinase.⁵ It is a vital trace

element, which is widely distributed in a variety of cells and tissues in different concentration level. The variation of copper ion concentration in neuronal cytoplasm is responsible for diseases like Alzheimer's and Parkinson's.⁶ The U.S. Environmental Protection Agency (EPA) has set the limit of copper in drinking water around 1.3 ppm ($\sim 20 \mu\text{M}$). The normal average concentration of copper in blood is around 15.7–23.6 μM .^{6c} In this context, significant progress has been made to develop good sensors for selective detection of Cu^{2+} however, practically most of these systems have limitations in the sense of cross sensitivity toward other metal ions, low water solubility, slow response, pH dependence, and a low fluorescence quantum yield in the aqueous medium.⁷ Moreover, it is known that copper induces fluorescence quenching due to its paramagnetic nature.⁸

Likewise, cyanide can also cause biological and environmental poisoning.⁹ The small amount of cyanide is lethal to human body¹⁰ due to its strong interaction with the active site of cytochrome a_3 ¹¹ that inhibits cellular respiration in mammalian cells. The sources of cyanide in water are discharge from chemical industries, metal mining processes, and waste water treatment facilities.⁹ Cyanide has also been used as a chemical warfare agent and even as a terror material.¹² The World Health Organization (WHO) has recommended concentration of cyanide in drinking water to be $\sim 1.9 \mu\text{M}$ for a healthy life.^{13b} Thus, detection of cyanide through coordination,¹⁴ covalent bonding^{12d} or displacement method^{13,15} has also received considerable interest among the scientific communities. Among the various sensing mechanisms, based on different phenomena of photophysics and chemical approaches Cu^{2+} displacement method recently become one of the important approaches due to its high

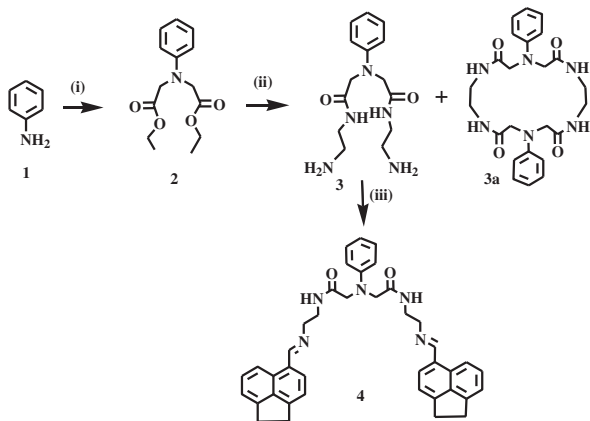
* Corresponding author. Tel.: +91 542 6702503; fax: +91 0542 2368127, +91 0542 2368175; e-mail addresses: amisra@bhu.ac.in, arvindmisra2003@yahoo.com (A. Misra).

affinity for cyanide to form stable $[\text{Cu}(\text{CN})_x]^{1-x}$ species in the medium.¹⁵ Thus, the ensemble based demetallization of copper by cyanide can be utilized as a good strategy to detect the cyanide in the medium. It is also because the d^9 electronic configuration of paramagnetic Cu^{2+} have strong binding affinity toward cyanide and the complexes with Cu^{2+} can recognize CN^- by ensuring high stabilization effects on the ligand field.¹⁶ Therefore, the design and synthesis of new systems that can display enhanced fluorescence upon interaction with metal ions/anions are in great demand and of the various optoelectronic techniques fluorescence spectroscopy has advantages as it offers high detection sensitivity and simplicity.¹⁷

The chelating groups like $-\text{C}=\text{N}$ and $-\text{C}=\text{O}$ exhibit high binding affinity to transition and post transition metal ions in comparison to alkali and alkaline earth metal ions.¹⁸ In addition to this there are few systems, which utilize strong affinity of cyanide for transition metals. In such systems, complexation of cyanide with transition metal, like Cu^{2+} results a change in the photophysical property of receptor and provide a method for detection. We herein present first report on the design and synthesis of an acenaphthene based scaffold for a sensitive and selective detection of Cu^{2+} through enhanced excimer fluorescence and detection of cyanide through copper displacement method in aqueous organic medium. The probe **4** consists of acenaphthene units of almost negligible fluorescence with amide and aldimine functions that has been utilized as a potential binding site for the ions. Upon interaction with Cu^{2+} the acenaphthyl units come close to each other and generate high excimer fluorescence,⁸ in which the acenaphthene units attained a stacked conformation, that ultimately leads to enhance intramolecular $\pi-\pi$ interaction.

2. Results and discussion

Scheme 1 describes the synthetic route of probe **4**. Aniline and α -bromoethylacetate in presence of KI and Na_2HPO_4 in acetonitrile (MeCN) were refluxed overnight under anhydrous condition to obtain compound **2** as a viscous liquid in $\sim 75\%$ yield. Compound **2** was constituted in ethanol and refluxed with ethylenediamine for 6 h to obtain compound **3** and **3a** (confirmed by ^1H NMR spectra), which were separated by column chromatography in ~ 37 and 51% yield, respectively. Acenaphthene was reacted with phosphorouschloride in N,N' -dimethylformamide (DMF) at 70°C to obtain 5-formylacenaphthene by a reported procedure,¹⁹ and was subsequently refluxed with **3** in ethanol at 80°C for 3 h to get a brown colored semisolid compound **4** in $\sim 76\%$ yield. The products were characterized by analytical and spectral data analysis (Fig. S1–9, Supplementary data).



Scheme 1. (i) $\text{BrCH}_2\text{COOEt}/\text{KI}/\text{Na}_2\text{HPO}_4/\text{CH}_3\text{CN}/\Delta$, (ii) ethylenediamine/EtOH/ Δ , (iii) 5-acenaphthenealdehyde/EtOH/ Δ .

2.1. Optical behavior of **4** with different cations

The UV–vis absorption spectrum of **4** ($5\ \mu\text{M}$) displayed a broad absorption band between ~ 280 and $340\ \text{nm}$ (at $\sim 340\ \text{nm}$, $\epsilon=27,000\ \text{M}^{-1}\ \text{cm}^{-1}$) in $\text{H}_2\text{O}/\text{MeCN}$ (8:2, v/v) solution. The binding behavior of **4** was investigated toward different metal ions by UV–visible and fluorescence spectroscopy. Upon interaction with different metal ions (10 equiv), such as Na^+ , K^+ , Ag^+ , Ca^{2+} , Co^{2+} , Ni^{2+} , Cu^{2+} , Zn^{2+} , Hg^{2+} , Ag^+ , Fe^{3+} , Pb^{2+} (as their nitrate salts) the broad absorption band of **4** upon interaction with Cu^{2+} ion disappeared and concomitantly a new transition band was appeared at $407\ \text{nm}$ (Fig. 1). The red shift observed in the absorption spectra may be attributed to an increase in intramolecular $\pi-\pi$ interaction between two acenaphthyl units as a result of coordination of Cu^{2+} through the amide and aldimine functional groups of **4** in ground state.^{8a} The other tested metal ions failed to exhibit any significant change in the absorption spectrum of **4** (Fig. 1).

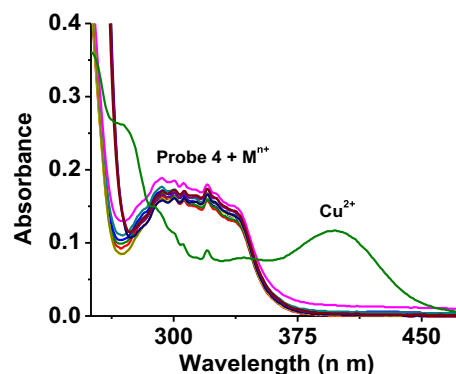


Fig. 1. Change in absorption spectra of **4** ($5\ \mu\text{M}$) upon addition of different metal ions (10 equiv) in $\text{H}_2\text{O}/\text{MeCN}$ (8:2, v/v).

The absorption titration experiment was performed to understand the binding affinity of **4** ($5\ \mu\text{M}$) with Cu^{2+} ion. Upon sequential addition of Cu^{2+} (0–3 equiv) to a solution of **4** the broad band centered at $340\ \text{nm}$ reduced gradually with the formation of a new transition band at $407\ \text{nm}$. An isosbestic point appeared at $348\ \text{nm}$ clearly suggested about the existence of more than one species in medium. Job's plot analysis revealed a 1:1 stoichiometry for a complexation between **4** and Cu^{2+} . An association constant estimated by Benesi–Hildebrand method²⁰ utilizing nonlinear fitting of absorption titration data and was found to be $K_{\text{assoc}}=3.22\times 10^5\ \text{M}^{-1}$ (Fig. 2).

The fluorescence spectrum of **4** ($5\ \mu\text{M}$) in $\text{H}_2\text{O}/\text{MeCN}$ (8:2, v/v) showed a very weak and broad monomer emission band in range of $380\text{--}420\ \text{nm}$, when excited at $340\ \text{nm}$. There was no band corresponding to excimer emission that means two acenaphthene units are not in stacked conformation. Among all the tested cations, **4** showed high selectivity toward copper metal ion whereas, insignificant change was observed upon interaction with other cations. Upon interaction with Cu^{2+} emission spectrum of **4** illustrated significant fluorescence enhancement, in which the weak emission band of monomer red shifted to appear at $507\ \text{nm}$ (Fig. 3) and color of solution changed from a non-fluorescent to fluorescent green under UV light (Inset, Fig. 3). The appearance of new emission band of relatively high emission intensity signifies the formation of a dimeric species in medium, in which two acenaphthene rings occupied the stacked conformation probably due to coordination of Cu^{2+} ion through the coordination sites available in form of amide and aldimine functional groups. Thus, it is worth to mention that copper induced a kind of driving force to bring two acenaphthyl rings in stacked conformation.

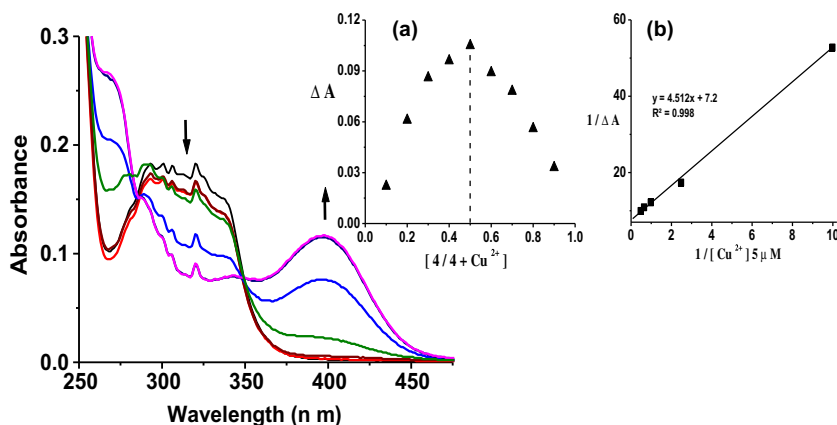


Fig. 2. Absorption titration spectra of **4** (5 μM) upon addition of Cu^{2+} ions (0–3 equiv) in $\text{H}_2\text{O}/\text{MeCN}$ (8:2, v/v). Inset (a) Job's plot and (b) Benesi–Hildebrand plot of **4** for Cu^{2+} .

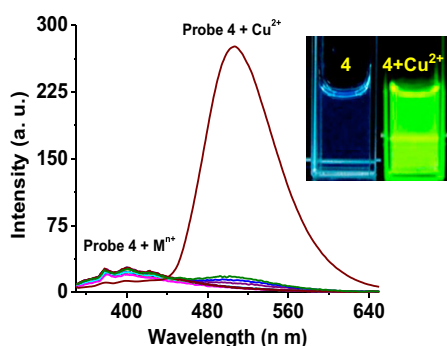


Fig. 3. Change in emission spectra of **4** (5 μM) upon addition of different metal ions (10 equiv) in $\text{H}_2\text{O}/\text{MeCN}$ (8:2, v/v). Inset shows the change in color under UV light.

The practical applicability of compound **4** as a selective fluorescent chemosensor for copper has been demonstrated by performing the competitive metal ion interference experiments. For that tested cations (10 equiv) were added to a solution of probable complex, $\mathbf{4}+\text{Cu}^{2+}$ and reversibly by the addition of Cu^{2+} ion to a solution of **4** containing excess of other metal ions (Fig. 4). No significant variation in excimer emission was observed in comparison to emission spectra of **4** in either condition. The absorption spectra upon addition of other tested cations illustrated insignificant change in absorption band of a complex $\mathbf{4}+\text{Cu}^{2+}$ centered at 407 nm (Fig. S10, Supplementary data). Thus, the experimental observation has suggested that compound **4** may be utilized as a potential fluorescent chemosensor for Cu^{2+} ion.

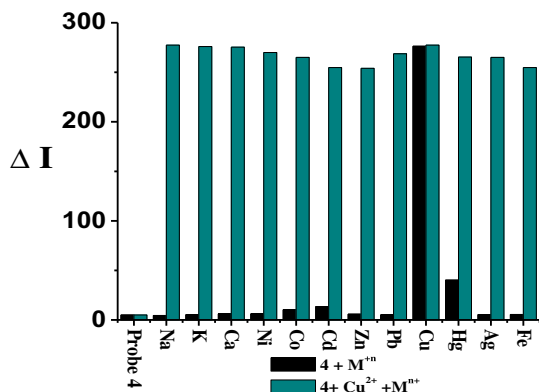


Fig. 4. Bar diagram illustrate the change in relative emission intensity of **4** (5 μM) and $\mathbf{4}+\text{Cu}^{2+}$ complex upon addition of competitive metal ions (10 equiv) at 507 nm in $\text{H}_2\text{O}/\text{MeCN}$ (8:2, v/v).

The fluorogenic affinity of **4** ($\Phi_4=0.0022$) with Cu^{2+} ions was evaluated by fluorescence titration experiment (Fig. 5). Upon increasing concentration of Cu^{2+} ions (0–3 equiv) to a solution of **4** relative fluorescence intensity increased significantly at 507 nm along with fluorescence enhancement factor (FEF) 147 whereas, the intensity of emission band at ~ 400 nm decreased ratiometrically with the formation of an isoemissive point at 439 nm. The quantum yield of a probable complex, $\mathbf{4}+\text{Cu}^{2+}$ was increased ($\Phi_{4+\text{Cu}^{2+}}=0.224$) and the color of solution appeared as fluorescent green under UV light. The high emission intensity observed at 507 nm is attributed to formation of intramolecular excimer²¹ led enhanced $\pi-\pi$ interaction between the two acenaphthene rings in consequence to complexation of Cu^{2+} ion through amide and aldimine functional groups. Job's plot analysis revealed consistently a 1:1 stoichiometry for a complexation between **4** and Cu^{2+} ions. The binding constant estimated from the fluorescence titration data was found to be $1.18 \times 10^5 \text{ M}^{-1}$. Moreover, a fluorescence intensity ratio plot⁴ obtained between the relative fluorescence intensity ratio, I_{400}/I_{507} and Cu^{2+} ion concentration suggested about the change in fluorescence intensity ratiometrically after the addition of 0.5 equiv of Cu^{2+} ion with a detection limit⁴ of $\sim 2.0 \mu\text{M}$ (Fig. S11, Supplementary data). The ESI-MS spectrum analysis of **4** and **3a** showed the molecular ions $[\text{MH}]^+$ peaks at m/z 622 and 467, respectively, (Fig. S5 and 9). Upon interaction between **4** and Cu^{2+} a new peak observed at m/z 684 $[\mathbf{4}+\text{Cu}]^+$ support the formation of a complex, $\mathbf{4}+\text{Cu}^{2+}$ in the medium and also about a 1:1 stoichiometry between probe **4** and Cu^{2+} (Fig. S12, Supplementary data).

Further, to examine the reversibility in complexation a strong chelating reagent, ethylene diaminetetraacetate (EDTA) was added (50 equiv) to a solution of probable complex, $\mathbf{4}-\text{Cu}^{2+}$. The observed red-shifted low energy absorption and emission bands of complex $\mathbf{4}+\text{Cu}^{2+}$ were disappeared consistently, with the generation of original bands at respective wavelengths. This may be attributed to formation of a strong $\text{EDTA}+\text{Cu}^{2+}$ complex in medium (Fig. S13, Supplementary data). Thus, the experimental observations have suggested about the reversible mode of complexation and potential application of probe **4** in the detection of copper in a repeated cycle.^{7d} Additionally, the fluorescence excitation spectra (Fig. S14, Supplementary data) were acquired to understand that the observed emission in case of complex, $\mathbf{4}+\text{Cu}^{2+}$ is due to excimer formation and also to ensure whether it is static or dynamic.^{7f} It is also because if a probe and its probable complex upon excitation corresponding to its emission bands do not show complete overlap in their excitation spectra then the respective observed emission is attributed to static excimer.^{7f} For that probe **4** and its complex, $\mathbf{4}-\text{Cu}^{2+}$ were excited at emission wavelengths 402 and 507 nm, respectively. The excitation spectra of $\mathbf{4}-\text{Cu}^{2+}$ showed formation of

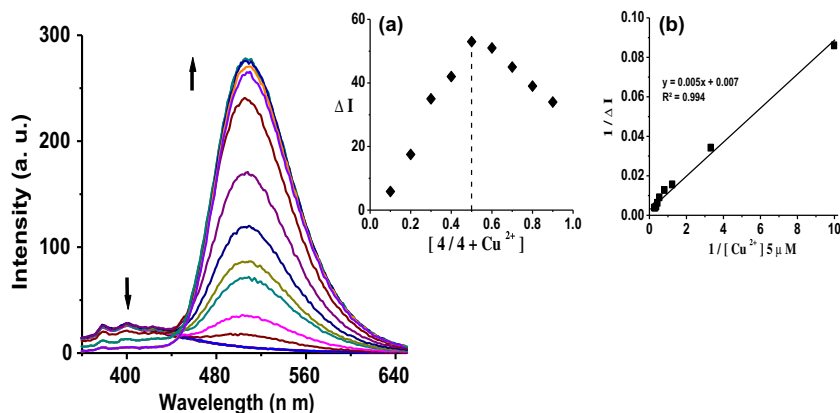
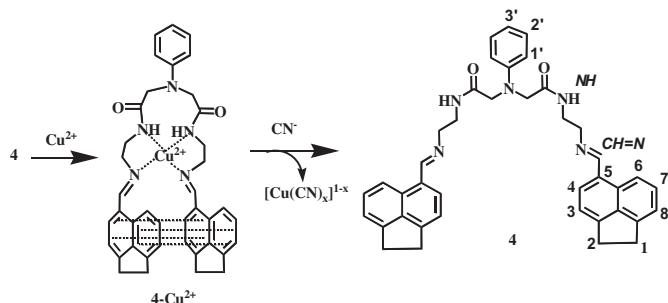


Fig. 5. Emission titration spectra of **4** (5 μM) upon addition of Cu^{2+} ions (0–3 equiv) Inset: (a) Job's plot and (b) Benesi–Hildebrand graph for **4** with Cu^{2+} ions in $\text{H}_2\text{O}/\text{MeCN}$ (8:2, v/v).

a new intense band centered ~ 400 nm whereas, no such band was observed when probe **4** was excited at 402/507 nm. Thus, clearly supporting that in the present sensing event the observed high emission intensity is attributed to Cu^{2+} induced static excimer fluorescence.

2.2. Mechanism of complexation between **4** and Cu^{2+}

The probable mechanism of complexation, as shown in Scheme 2 was confirmed by ^1H NMR spectra of **4** in the presence of Cu^{2+} ions (0.5, 1 and 2 equiv). The ^1H NMR spectrum of **4** showed resonances for H1' and H3' proton at δ 6.46 ppm and a triplet for H2' at δ 6.97 ppm. The H4 proton of acenaphthene unit merged with aldimine ($-\text{C}=\text{NH}$) proton to appear at δ 8.71 ppm whereas, a broad signal appeared at δ 7.95 ppm may be attributed to amide ($-\text{CONH}$) function proton. The other aromatic protons were appeared between δ 7.25–7.76 ppm. Upon addition of 0.5–2.0 equiv of Cu^{2+} ions to a solution of **4** a significant downfield shift in the resonances of amide and aldimine protons, $\Delta\delta=0.18$ and 1.56 ppm, respectively, were observed and resonances of acenaphthyl ring protons become broadened (Fig. 6). Therefore, suggested about the coordination of Cu^{2+} with both amide and aldimine functions of **4** and that enforce acenaphthene rings to occupy stacked conformation. Consequently, enhanced intramolecular $\pi-\pi$ interaction led to observe intense excimer fluorescence⁷ and a naked-eye sensitive green color was appeared in the medium.



Scheme 2. Proposed mechanism for interaction of **4** with the Cu^{2+} and CN^- ions.

2.3. Quantum chemical calculations

Further to support our assumptions, experimental observations and possible structural changes we have performed quantum chemical calculations. The geometry optimization were performed

for probe **4** and its complex, **4**+ Cu^{2+} using density functional theory (DFT) method as implemented in Gaussian 03 suits of program.²² All the calculations were performed using B3LYP density functional theory method, a hybrid version of DFT and Hartree–Fock (HF) methods, in which the exchange energy from Becke's exchange functional is combined with the exact energy from Hartree–Fock theory along with the component exchange and correlation functionals, Becke's three parameters define the hybrid functional, specifying the extent of the exact exchange mixed in. We have used a 6-31G(d,p) basis set for all the atoms except metal atom (Cu^{2+}), for which an effective core LanL2DZ basis set was chosen. A frequency calculation for the metal complex was performed to make sure that the optimized structure is a real minimum. The optimized structure of **4**- Cu^{2+} complex (II and IV of Fig. 7) indicates that Cu^{2+} ion coordinated with nitrogen-donor atom of aldimine and amide functions of **4** in square planer conformation. Due to complexation of **4** with Cu^{2+} ion the acenaphthene moiety come closer while in probe **4** acenaphthene units remained apart from each other (I and III of Fig. 7). The DFT optimized structure showed two bond length between the Cu^{2+} and N-atom of amide are 2.45, 2.65 Å and between the Cu^{2+} and N-atom of aldimine are both of 1.92 Å.

2.4. Optical behavior of complex **4**- Cu^{2+} with different anions and CN^- anion

Among the various sensing approaches a metal chelate based sensing method of copper complexes can be utilized to device a good fluorescent sensor for CN^- because of high affinity of cyanide and copper to produce stable $[\text{Cu}(\text{CN})_x]^{1-x}$ species in a medium.¹⁵ To address this possibility we investigated optical behavior of **4**- Cu^{2+} complex (5 μM) in the presence of different anions in $\text{H}_2\text{O}/\text{MeCN}$ solution (8:2, v/v). Upon addition of different anions (10 equiv), such as F^- , Cl^- , Br^- , I^- , SCN^- , H_2PO_4^- , CN^- , AcO^- , PO_4^{3-} , S^{2-} (as their sodium salts) to a solution of **4**- Cu^{2+} (5 μM) significant change in the optical properties was observed only upon interaction with CN^- ion, in which, both the absorption and emission spectra of **4** rejuvenated almost completely. Some sort of interaction was also observed with S^{2-} ion, which interacts with **4**- Cu^{2+} complex and causes $\sim 40\%$ fluorescence quenching (Fig. 8, S15).

The binding affinity of a complex, **4**- Cu^{2+} with CN^- ion was estimated by performing absorption and emission titration experiments (Fig. 9). Upon a sequential addition of CN^- (0–4 equiv) to a solution of **4**- Cu^{2+} absorption band centered at ~ 400 nm decreased gradually and a new broad band around ~ 340 nm was generated with the formation of an isosbestic point at 350 nm

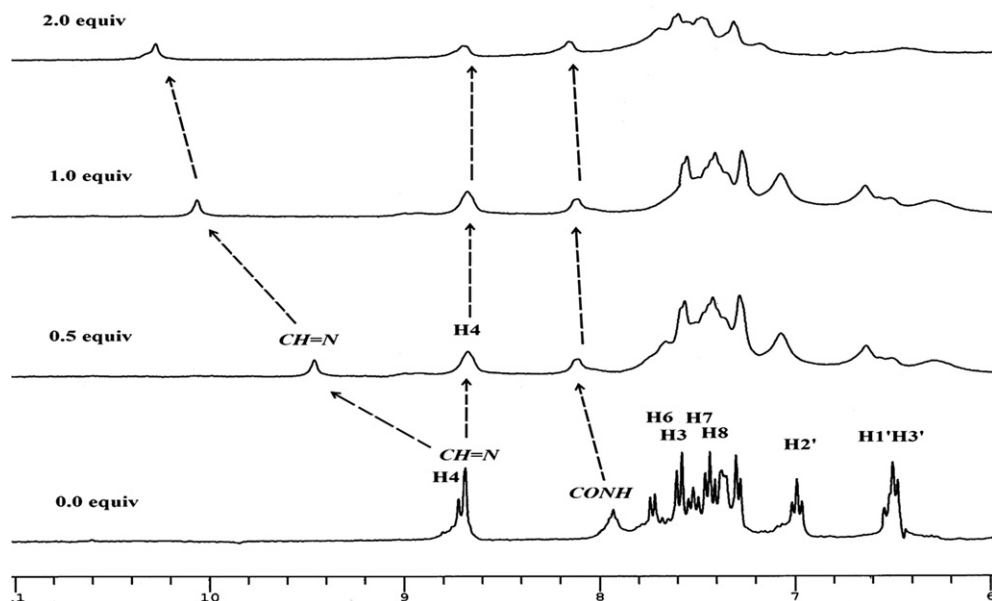


Fig. 6. Change in ^1H NMR spectra of **4** ($c=1.02\times 10^{-2}$ M) upon addition with Cu^{2+} (0.5, 1 and 2 equiv) in $\text{DMSO-}d_6$.

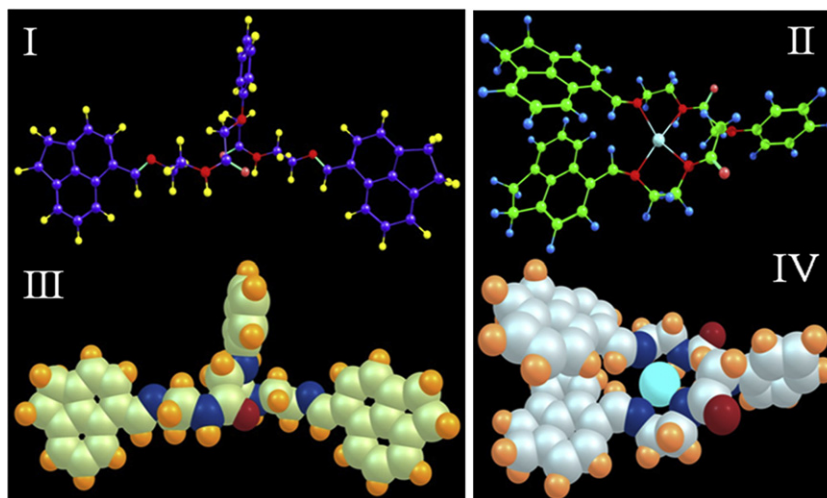


Fig. 7. DFT optimized structure of **4** and 4-Cu^{2+} complex.

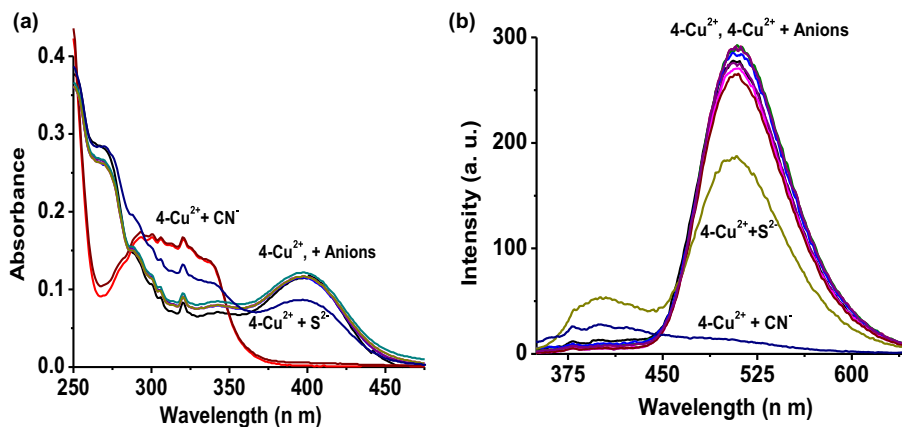


Fig. 8. Change in (a) absorption and (b) emission spectra of 4-Cu^{2+} ($5\ \mu\text{M}$) upon addition of different anions (10 equiv) in $\text{H}_2\text{O}/\text{MeCN}$ (8:2, v/v).

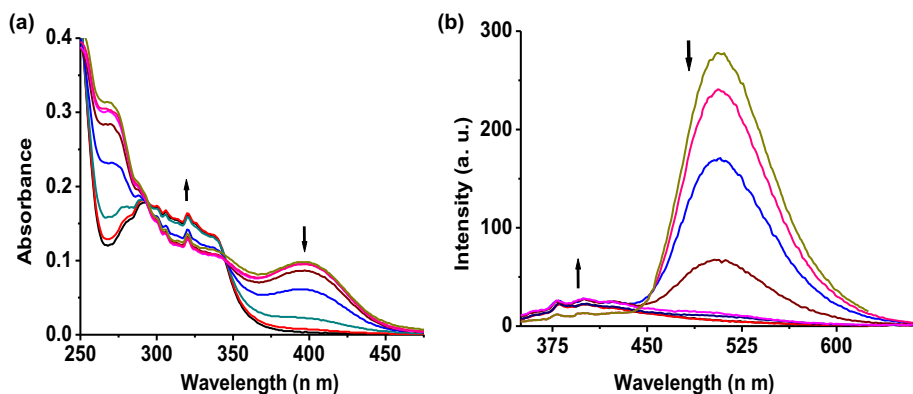


Fig. 9. (a) UV-vis absorption and (b) fluorescence titration spectra of **4**-Cu²⁺ complex (5 μM) upon addition of CN⁻ ions (0–4 equiv) in H₂O/MeCN (8:2, v/v).

(Fig. 9a). Similarly, fluorescence intensity of emission band centered at 507 nm decreased ratiometrically while the relative intensity of an emission band, centered at ~400 nm increased along with formation of an isoemissive point at 437 nm (Fig. 9b). The color of solution readily visible to the naked-eye was changed from a fluorescent green to non-fluorescent. The absorption and fluorescence titration experiment data were utilized to estimate binding constant of CN⁻ ion with a complex, **4**-Cu²⁺ and were found to be 1.32×10^6 and 2.05×10^6 M⁻¹, respectively. The detection limit of **4**-Cu²⁺ complex for CN⁻ ion was estimated and was found to be 1 μM (i.e., 25 ppb). The high sensitivity to the maximum permissible level in drinking water, 1.9 ppm recommended by WHO authenticate the novelty of present mode of CN⁻ sensing mechanism obviously attributed to demetallization of a probable complex, **4**+Cu²⁺ by cyanide and formation of [Cu(CN)_x]^{1-x} species in the medium as shown in Scheme 2.

The stability constants (*K*) for the formation of probable different complex, [Cu(CN)_x]^{1-x} species^{15b} in the medium are [Cu(CN)₂]⁻= 1.00×10^{24} ; and [Cu(CN)₄]³⁻= 2.0×10^{30} . Since, the estimated association constant of a complex between **4** and Cu²⁺ was comparatively low, $K_{\text{assoc}}=1.18 \times 10^5$ M⁻¹ than the stability constant of copper and cyanide ions it is reasonable to understand that upon addition of CN⁻ to a solution of complex, **4**+Cu²⁺ led to a formation of [Cu(CN)_x]^{1-x} species in the medium, due to which modulation in both absorption and emission spectra were observed.

2.5. Interaction of **4** with CN⁻ anion

Compound **4** contains amide group and it is rationally concluded that the amide unit reasonably form complexes with different anions probably through hydrogen bonding between anions and amide -NH fragment.²³ Therefore, we intended to investigate binding affinity of **4** toward different anions, such as, F⁻, Cl⁻, Br⁻, I⁻, SCN⁻, H₂PO₄⁻, CN⁻, NO₃⁻, AcO⁻, S²⁻, PO₄³⁻ (as their sodium salts) in H₂O/MeCN (8:2, v/v) solution. The absorption spectrum of **4** showed insignificant change with different anions (Fig. S16). Conversely, the emission spectra upon addition of different anions (50 equiv) to a solution of **4** (5 μM) exhibited significant fluorescence enhancement only upon interaction with CN⁻. A new emission band was appeared at 452 nm and the color of solution appeared blue. This may be probably attributed to formation of excimer up to lesser extent relatively, in comparison to Cu²⁺, upon an interaction of CN⁻ with amide function of **4** through H-bonding interaction whereas, insignificant spectral changes were observed upon interaction with other tested anions (Fig. 10). A competitive anion interaction studies were also performed to understand the selectivity of **4** with cyanide anion. Upon addition of cyanide to a solution of **4** containing different anions and reversibly addition

of different anions to a solution of **4**+CN⁻ the relative emission intensity of **4**+CN⁻ remained unaltered (Fig. 11).

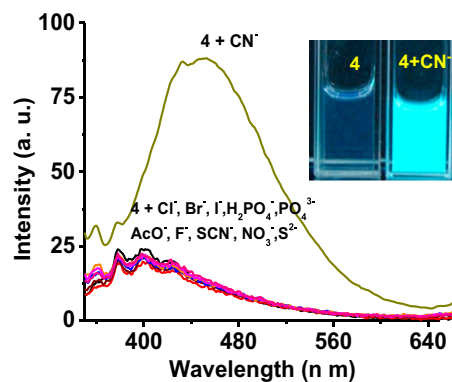


Fig. 10. Change in emission spectra of **4** (5 μM) upon addition of different anions (50 equiv) in H₂O/MeCN (8:2, v/v).

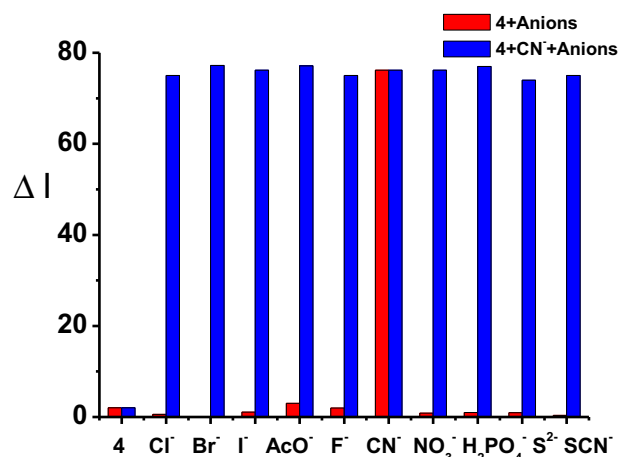
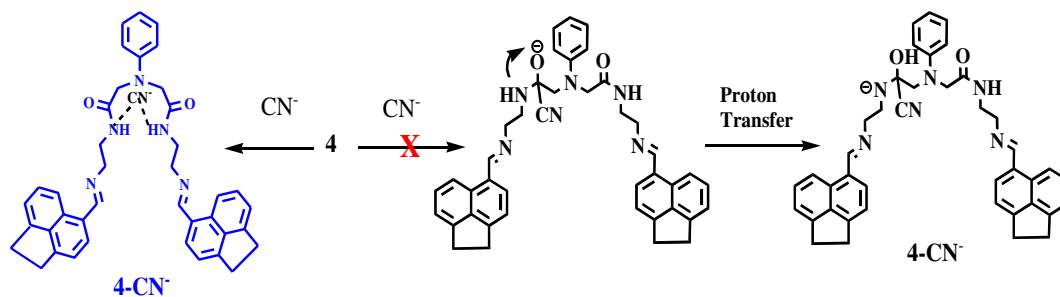


Fig. 11. Bar diagram illustrate the change in relative emission intensity of **4** (5 μM) (red in color) and **4**-CN⁻ complex (blue in color) upon addition of competitive anions (50 equiv) at 452 nm in H₂O/MeCN (8:2, v/v).

Contrary, one can also speculate about an opportunity of nucleophilic addition reaction between **4** and cyanide, in which, cyanide can approach -C=O group of amide functionality to form a new charged cyanohydrin species¹⁵ in the medium. A probability for such type of chemical reaction is depicted in Scheme 3. Our this speculation was based on speculation of much lower intrinsic hydration energy of CN⁻ ($\Delta H_{\text{hyd}}=-67$ kJ mol⁻¹) in comparison to very



Scheme 3. Probable mechanism of interaction between probe, **4** and CN^- anion.

high solvation energy for other anions, for instance, F^- ($\Delta H_{\text{hyd}} = -505 \text{ kJ mol}^{-1}$), Cl^- ($\Delta H_{\text{hyd}} = -363 \text{ kJ mol}^{-1}$), Br^- ($\Delta H_{\text{hyd}} = -336 \text{ kJ mol}^{-1}$), I^- ($\Delta H_{\text{hyd}} = -295 \text{ kJ mol}^{-1}$), CH_3COO^- ($\Delta H_{\text{hyd}} = -375 \text{ kJ mol}^{-1}$), and H_2PO_4^- ($\Delta H_{\text{hyd}} = -260 \text{ kJ mol}^{-1}$) in $\text{H}_2\text{O}/\text{MeCN}$ (7:1, v/v) solution.²⁴

To establish the actual mechanism, ^1H NMR spectral data of **4** in the presence of cyanide was acquired in $\text{DMSO}-d_6$. Upon addition of 2–5 equiv of CN^- to a solution of **4** a broad resonance attributed to amide ($-\text{CO NH}$) function, at δ 7.95 ppm shifted downfield to appear at δ 8.19 ppm ($\Delta\delta = 1.16 \text{ ppm}$). The $\text{H}1'$ and $\text{H}3'$ protons were separated to appear at δ 6.45 and 6.53 ppm, respectively, whereas, a marginal change in the resonances of aromatic ring protons as well as in aldimine ($-\text{C}=\text{NH}$) proton, at δ 8.71 ppm were observed (Fig. 12). Additionally, the ^1H NMR spectrum of **4** showed doublet at δ 3.6 ($J = 5.7 \text{ Hz}$) and singlet at δ 3.68 ppm attributable to methylene protons ($-\text{CH}_2\text{CH}_2-$) and proton neighboring to carbonyl function

constant estimated from nonlinear fitting of fluorescence titration data was found to be $K_{\text{assoc}} = 2.06 \times 10^4 \text{ M}^{-1}$ (Fig. 13). Comparatively, the observed association constants for complex, **4**+ CN^- was relatively low than of **4**+ Cu^{2+} and **4**+ Cu^{2+} + CN^- . Thus, clearly suggesting about the interaction between **4** and cyanide through H-bonding rather than a possibility of nucleophilic addition reaction of cyanide on to the imine, $-\text{C}=\text{NH}$ as well as on carbonyl, $-\text{C}=\text{O}$ group of amide functional units. Further, to rule out the expected probability for a nucleophilic addition reaction, Cu^{2+} was added to a solution of probable complex, **4**- CN^- . Fluorescence quenching occurred, in which the intensity of the emission band, centered at 452 nm diminished completely and the emission spectra almost same to probe **4** was rejuvenated (Fig. S20). This may be attributed to the formation of stable species, $[\text{Cu}(\text{CN})_x]^{1-x}$ and free probe **4** in the medium. Moreover, upon interaction with CN^- if the speculated chemical reaction, leading to formation of cyanohydrin derivative was accurate,

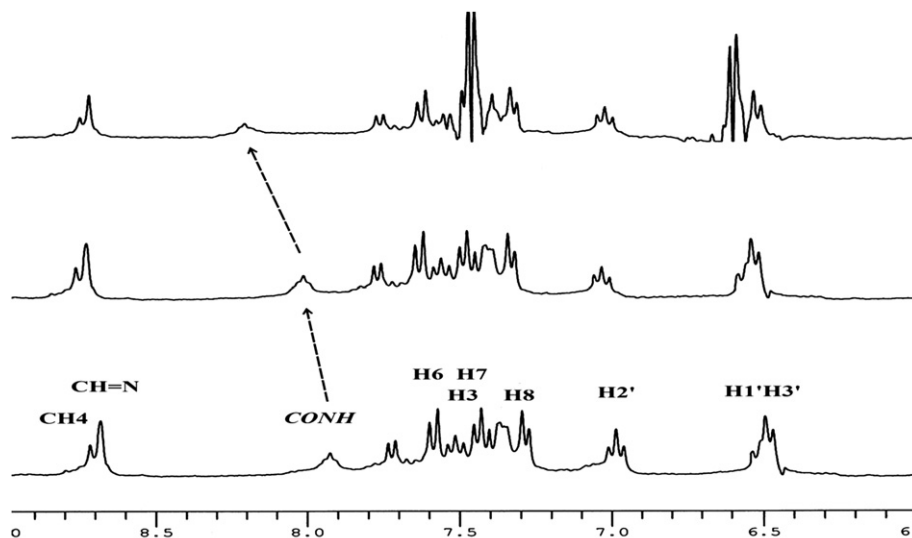


Fig. 12. ^1H NMR titration spectra of **4** ($c = 1.02 \times 10^{-2} \text{ M}$) upon addition of CN^- (2, 5 equiv) in $\text{DMSO}-d_6$.

of amide group, respectively, (Fig. S17). Upon interaction with CN^- almost insignificant downfield chemical shift, rather than any upfield shift was observed at the corresponding resonances (Fig. S18 and 19). Thus, suggesting that interaction of cyanide is primarily through hydrogen bonding with the amide fragment of probe **4** rather than speculated chemical reaction, as shown in Scheme 3.

Further, to elucidate binding affinity of **4** for CN^- fluorescence titration experiment was carried out. Upon addition of CN^- anions (0–50 equiv) to a solution of **4** relative fluorescence intensity was enhanced gradually (FEF=8.2) and the quantum yield was increased ~ 34 times ($\Phi_{4-\text{CN}^-} = 0.0754$), which was relatively less in comparison to **4**+ Cu^{2+} . Job's plot analysis revealed a 1:1 stoichiometry for a probable complexation between **4** and CN^- . The association

then upon addition of Cu^{2+} to a solution of **4**- CN^- complex there might be possibility for generation of a new band in the absorption spectra and accordingly change in the fluorescence behavior. However, beyond our speculation no such significant spectral changes were observed. Thus, fluorescence, UV–vis absorption and ^1H NMR spectra exclusively validated the interaction of **4** with CN^- through H-bonding²⁵ and ruled out our assumption for a possible nucleophilic addition reaction leading to formation of possible cyanohydrin derivative in the medium. This was further confirmed by ESI-MS data analysis, in which no new signal corresponding to generation of cyanohydrin derivative was observed (Fig. S21).

Further, to strengthen our hypothesis for a probable mode of interaction with Cu^{2+} and CN^- ions and involvement of excimer

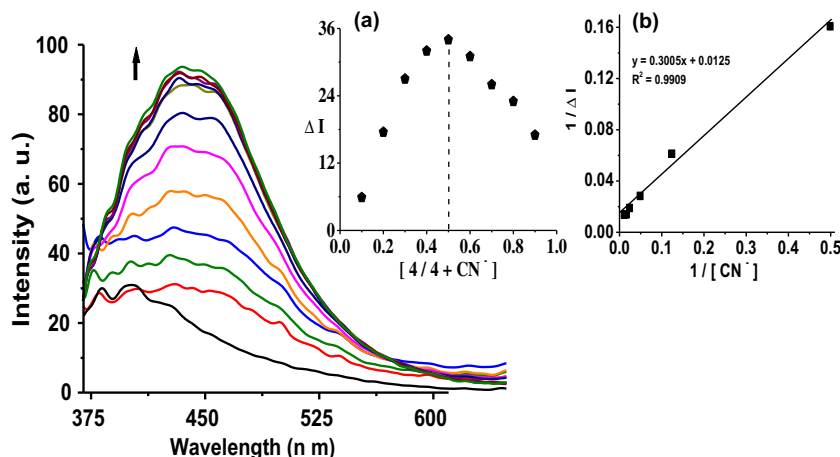


Fig. 13. Emission titration spectra of probe **4** (5 μM) upon addition of different equiv of CN^- ions (0–50 equiv) in $\text{H}_2\text{O}/\text{MeCN}$ (8:2, v/v). Inset: (a) Job's plot and (b) Benesi–Hildebrand graph of probe **4** upon addition of CN^- ions in $\text{H}_2\text{O}/\text{MeCN}$ (8:2, v/v).

fluorescence upon interaction of **4** with Cu^{2+} and CN^- derivative, **3a** (5 μM) was utilized as a model compound. The affinity of **3a** toward different cations (50 equiv) and anions (100 equiv) was tested under the same experimental condition. Compound **3a** displayed a weak monomer emission at 425 nm, when excited at 340 nm. In contrast to **4** compound **3a** upon interaction with different cations exhibited fluorescence quenching with Cu^{2+} while oppositely, illustrated fluorescent enhancement with CN^- , in which, the emission spectra displayed a bathochromic shift of ~ 60 nm to appear at 485 nm (Figs. S22 and 23, Supplementary data). The association constants estimated for a possible complexation between **3a** and $\text{Cu}^{2+}/\text{CN}^-$ ions in a 1:1 stoichiometry, respectively, were found to be $7.26 \times 10^3 \text{ M}^{-1}$ and $4.32 \times 10^4 \text{ M}^{-1}$ (Fig. S24, Supplementary data). Moreover, upon addition of CN^- (40 equiv) to a probable complex of **3a**- Cu^{2+} and conversely, Cu^{2+} (40 equiv) to a solution of probable complex, **3a**- CN^- the relative emission intensity revived, which was almost close to the intensity signal of **3a** (Fig. S25, Supplementary data). Thus, the observed optical behavior clearly suggested about the detection of cyanide via Cu^{2+} displacement approach and also about the interaction of cyanide with derivative **3a** through the H-bonding interaction.

3. Conclusion

Conclusively, a new simple probe **4** was designed and developed, which was capable to detect Cu^{2+} ion through the enhanced fluorescence intensity ratiometrically. The interaction of copper with the amide and aldimine functional groups encouraged excimer formation by reducing the distance between the two acenaphthyl rings and increasing the π - π interaction, consequently. The change in color of solution from non-fluorescent to a fluorescent green was readily distinguishable to naked eye. On the other hand, interaction of **4**- Cu^{2+} with cyanide ion revealed fluorescence quenching due to a strong copper-cyanide affinity leading to the formation of stable $[\text{Cu}(\text{CN})_x]^{1-x}$ species. The probe **4** also exhibited sensing of CN^- in aqueous-MeCN solution, in which fluorescence enhancement was observed at ~ 452 nm.

4. Experimental

4.1. Instrumentation

The absorption and emission spectra were recorded at room temperature on a Shimadzu 1700 spectrophotometer using a quartz cuvette (path length=1 cm) and CARY Eclipse (VARIAN) fluorescence spectrophotometer at 600 V PMT keeping a constant

band width of 5 nm/5 nm for both excitation and emission spectra, respectively. FTIR spectra (KBr pellets) were recorded on a Perkin Elmer Spectrum spectrometer. The ^1H and ^{13}C NMR spectra (chemical shifts in δ ppm) were recorded on a JEOL AL 300 FT-NMR (300 MHz) spectrometer, using tetramethylsilane (TMS) as an internal standard. Mass spectra were recorded on a Micromass Quattro II spectrometer. Elemental analysis was carried out on CE-440 CHN Analyzer (Exeter Analytical Inc.).

4.2. Association constant/binding constant (K_{assoc})

The association constants have been calculated by non-linear fitting of the spectroscopic titration curve by using Benesi–Hildebrand method employing following equations 1 for 1:1 stoichiometry.

$$1/(I - I_0) = 1/(I - I_f) + 1/K(I - I_f)[M] \quad (1)$$

Where, K is the association constant, I is fluorescence intensity or absorbance of free fluorescent probe, I_0 is the observed fluorescence intensity or absorbance of the complex (**Probe + ions**) and I_f is the fluorescence intensity or absorbance at saturation.

4.3. Quantum yields (Φ)

The quantum yields were estimated in acetonitrile solution by secondary method¹ using Eq. 2 with respect to the quinine sulfate ($\Phi=0.55$ in 0.1 M H_2SO_4) as standard.

$$Q = Q_R \cdot (I/I_R) \cdot (OD_R/OD) \cdot (n^2/n_R^2) \quad (2)$$

Where, Q is the quantum yield, I is integrated area corresponding to the fluorescence intensity, OD is optical density, and n is the refractive index. The subscript R refers to the reference fluorophore of known quantum yield.

4.4. Synthesis and characterization of probe **4**

4.4.1. Synthesis of derivative 2. To the mixture of aniline (0.93 g, 10 mmol), Na_2HPO_4 (2.84 g, 20 mmol), and KI (1.66 g, 10 mmol) in anhydrous acetonitrile (MeCN), α -bromoethylacetate (5.56 ml, 50 mmol) was added. The reaction mixture was refluxed overnight under nitrogen atmosphere. After completion of reaction (as monitored on TLC) solvent was evaporated to dryness under reduced pressure, and cold water was added to it and then extracted with chloroform. The organic layer was separated and dried over anhydrous Na_2SO_4 . Filtered and chloroform was evaporated under

reduced pressure to obtain a viscous liquid (1.98 g, 75%). R_f (CHCl_3) 0.61; $^1\text{H NMR}$ (300 MHz, CDCl_3) δ (ppm): 7.21 (t, 2H, $J=7.8$, 7.5 Hz), 6.80 (m, 1H), 6.62 (d, 2H, $J=7.8$ Hz), 4.27 (m, 4H), 3.89 (s, 4H), 1.32 (t, 6H, $J=6.9$, 6.9 Hz).

4.4.2. Synthesis of derivative 3 and 3a. To a warm solution of **2** (1.33 g, 5 mmol) in ethanol (10 ml), ethylenediamine (5 ml) was added and refluxed the reaction mixture for 5 h. After completion of the reaction (as monitored on TLC), solvent was evaporated under reduced pressure to obtain a yellow color viscous oil. The cold water was added to the reaction mixture and product was extracted with CHCl_3 and separated by column chromatography to get viscous oil. For **3** (0.52 g, 37%); R_f (CHCl_3) 0.1; $^1\text{H NMR}$ (300 MHz, CDCl_3) δ (ppm): 7.24 (t, 2H, $J=7.8$, 7.8 Hz), 7.02 (br, 2H), 6.83 (t, 1H, $J=7.2$, 7.5 Hz), 6.63 (d, 2H, $J=8.1$ Hz), 4.26 (br), 3.82 (d, 4H, $J=4.8$ Hz), 3.35 (m, 4H), 2.81 (m, 4H).

For **3a** (1.18 g, 51%); R_f (CHCl_3) 0.5; $^1\text{H NMR}$ (300 MHz, CDCl_3) δ (ppm): 7.21 (m, 2H), 7.04 (br, 2H), 6.80 (m, 1H), 6.63 (d, 2H, $J=7.5$ Hz), 3.81 (s, 4H), 3.42 (s, 4H); ESI-MS (**3a**): m/z 194 (100), 467.2 (70%, MH^+).

4.4.3. Synthesis of probe 4. To a solution of **3** (0.29 g, 1 mmol) in ethanol (10 ml), 5-formylacenaphthene (0.36 g, 2 mmol) was added and reaction mixture was refluxed for 3 h and monitored (on TLC). Solvent was reduced under vacuum and cold water was added to the reaction mixture. The precipitate so obtained was filtered and dried to give brown color semisolid compound (0.47 g, 76%). R_f (CHCl_3) 0.5; $^1\text{H NMR}$ (300 MHz, CDCl_3) δ (ppm): 8.60 (s, 2H), 8.54 (d, 2H, $J=8.1$ Hz), 7.58 (m, 4H), 7.48 (m, 2H), 7.33 (m, 4H), 7.12 (t, 2H, $J=7.8$, 7.5 Hz), 6.74 (t, 1H, $J=7.2$, 6.9 Hz), 6.54 (d, 2H, $J=7.8$ Hz), 3.76 (s, 4H), 3.72 (t, 4H, $J=4.8$, 4.8 Hz), 3.39 (m, 12H); $^{13}\text{C NMR}$ (75 MHz, CDCl_3) δ (ppm): 30.2, 39.9, 48.8, 61.2, 113.1, 118.7, 118.9, 119.1, 119.8, 120.6, 122.1, 127.4, 127.7, 129.3, 131.5, 132.1, 139.5, 145.9, 146.1, 147.0, 149.9, 162.9, 192.9; FTIR (KBr) ν_{max} (cm^{-1}) 3400, 2923, 1663, 1623, 1601, 1503, 1442, 1313, 1260, 838, 749; Anal. Calcd For $\text{C}_{40}\text{H}_{39}\text{N}_5\text{O}_2$: C, 77.27; H, 6.32; N, 11.26%. Found: C, 77.17; H, 6.70; N, 11.32%; ESI-MS (**4**): m/z 358 (70), 591 (22), 622.3 (100%, MH^+).

4.4.4. Synthesis of 5-formylacenaphthene. To a solution of acenaphthene (10 mmol, 1.54 g) in N,N' -dimethylformamide (26 mmol, 2 ml) POCl_3 (18 mmol, 1.6 ml) was added dropwise over 15 min with stirring at room temperature. After complete addition of POCl_3 the reaction was heated at 70 °C for 3 h and then allowed to cool in an ice bath. The reaction mixture was neutralised with sodium acetate solution (10 g in 18 ml of water) and left for precipitation. The precipitate was filtered followed by washing with water and dried in air to get the brown colored solid (5.7 mmol, 57%). Mp 103–105 °C; R_f (20% EtOAc/hexane) 0.6; $^1\text{H NMR}$ (300 MHz, CDCl_3) δ (ppm): 10.29 (s, 1H, CHO), 8.82 (d, 1H, $J=8.4$ Hz), 7.96 (d, 1H, $J=7.2$ Hz), 7.68 (t, 1H, $J=7.2$, 8.4 Hz), 7.43 (d, 2H, $J=6.6$ Hz), 3.45 (s, 4H, CH_2); FTIR (KBr) ν_{max} (cm^{-1}) 3047, 2927, 2773, 1665, 1550, 1445, 1340, 1251, 1166, 1047, 838, 749.

Acknowledgements

The authors are thankful to the Council of Scientific and Industrial Research (CSIR), New Delhi for financial support and fellowships (to M.S., S.S.R., P.S.) and UGC (R.A.) to carry out research work. Authors are also thankful to SAIF CDRI, Lucknow for providing ESI-MS spectral data.

Supplementary data

^1H , ^{13}C NMR, FTIR, ESI-MS, fluorescence, absorption spectral data. Supplementary data related to this article can be found online at <http://dx.doi.org/10.1016/j.tet.2012.08.052>.

References and notes

- (a) Yoon, J.; Kim, S. K.; Singh, N. J.; Kim, K. S. *Chem. Soc. Rev.* **2006**, 35, 355; (b) Czarnik, A. W. Ed.; American Chemical Society: Washington, DC, 1992. (c) Gunnlaugsson, T.; Glynn, M.; Tocci, G. M.; Kruger, P. E.; Pfeffer, F. M. *Coord. Chem. Rev.* **2006**, 250, 3094.
- (a) Zhang, J. F.; Zhou, Y.; Yoon, J.; Kim, J. S. *Chem. Soc. Rev.* **2011**, 40, 3416; (b) Wu, J.; Liu, W.; Ge, J.; Zhang, H.; Wang, P. *Chem. Soc. Rev.* **2011**, 40, 3483; (c) Kim, H. N.; Guo, Z.; Zhu, W.; Yoon, J.; Tian, H. *Chem. Soc. Rev.* **2011**, 40, 79.
- (a) Chen, X.; Pradhan, T.; Wang, F.; Kim, J. S.; Yoon, J. *Chem. Rev.* **2012**, 112, 1910; (b) Lodeiro, C.; Capelo, J. L.; Mejuto, J. C.; Oliveira, E.; Santos, H. M.; Pedras, B.; Nunez, C. *Chem. Soc. Rev.* **2010**, 39, 2948; (c) Qian, X.; Xiao, Y.; Xu, Y.; Guo, X.; Qiana, J.; Zhu, W. *Chem. Commun.* **2010**, 6418.
- Gryniewicz, G.; Poenie, M.; Tsien, R. Y. *J. Biol. Chem.* **1985**, 260, 3440.
- Kramer, R. *Angew. Chem., Int. Ed.* **1998**, 37, 772.
- (a) Multhaup, G.; Schlicksupp, A.; Hesse, L.; Behr, D.; Ruppert, T.; Masters, C. L.; Beyreuther, K. *Science* **1996**, 271, 1406; (b) Lovstad, R. A. *Biometals* **2004**, 17, 111; (c) Tak, W. T.; Yoon, S. C. *KSN* **2001**, 20, 863.
- (a) Zhou, Y.; Wang, F.; Kim, Y.; Kim, S.-J.; Yoon, J. *Org. Lett.* **2009**, 11, 4442; (b) Mu, H.; Gong, R.; Ma, Q.; Sun, Y.; Fu, E. *Tetrahedron Lett.* **2007**, 48, 5525; (c) Xu, Z.; Yoon, J.; Spring, D. R. *Chem. Commun.* **2010**, 46, 2563; (d) Martinez, R.; Espinosa, A.; Tarraga, A.; Molina, P. *Tetrahedron* **2010**, 66, 3662; (e) Misra, A.; Shahid, M. *J. Phys. Chem. C* **2010**, 114, 16726; (f) Manandhar, E.; Wallace, K. J. *Inorg. Chim. Acta* **2012**, 381, 15.
- (a) Jung, H.; Park, M.; Han, D.; Kim, E.; Lee, C.; Ham, S.; Kim, J. S. *Org. Lett.* **2009**, 11, 3378; (b) Kim, H.; Hong, J.; Hong, A.; Ham, S.; Lee, J.; Kim, J. S. *Org. Lett.* **2008**, 10, 1963.
- (a) Kulig, K. W. *Cyanide Toxicity*; U.S. Department of Health and Human Services: Atlanta, GA, 1991.
- Muir, G. D. *Hazards in the Chemical Laboratory*; The Royal Society of Chemistry: London, UK, 1977.
- Cyanide in Biology*; Vennesland, B., Comm, E. F., Knowlton, J., Westly, J., Wissing, F., Eds.; Academic: London, 1981.
- (a) Young, C.; Tidwell, L.; Anderson, C. *Cyanide: Social, Industrial, and Economic Aspects*; Minerals, Metals, and Materials Society: Warrendale, 2001; (b) Johnson, J. D.; Meisenheimer, T. L.; Isom, G. E. *Toxicol. Appl. Pharmacol.* **1986**, 84, 464; (c) Koenig, R. *Science* **2000**, 287, 1737; (d) Kim, H. J.; Lee, H.; Lee, J. H.; Choi, D. H.; Jung, J. H.; Kim, J. S. *Chem. Commun.* **2011**, 10918.
- (a) Miller, G. C.; Pritsos, A. *Cyanide: Social, Industrial and Economic Aspects*; Proceedings of the TMS Annual Meeting: 2001; p 73; (b) Guidelines for Drinking-Water Quality; World Health Organization: Geneva, Switzerland, 1996.
- Zou, Q.; Li, X.; Zhang, J.; Zhou, J.; Sun, B.; Tian, H. *Chem. Commun.* **2012**, 2095.
- (a) Lou, X.; Qiang, L.; Qin, J.; Li, Z. *Appl. Mater. Interfaces* **2009**, 1, 2529; (b) Song, T.; Xu, J.; Cheng, G. *Inorganic Chemistry*; Higher Education: Beijing, 2004; (c) Xu, Z.; Chen, X.; Kim, H. N.; Yoon, J. *Chem. Soc. Rev.* **2010**, 39, 127; (d) Xu, Z.; Pan, J.; Spring, D. R.; Cui, J.; Yoon, J. *Tetrahedron* **2010**, 66, 1678.
- (a) Huang, X. M.; Guo, Z. Q.; Zhu, W. H.; Xie, Y. S.; Tian, H. *Chem. Commun.* **2008**, 5143; (b) Zhang, J. F.; Kim, S.; Han, J. H.; Lee, S.-J.; Pradhan, T.; Cao, Q. Y.; Lee, S. J.; Kang, C.; Kim, J. S. *Org. Lett.* **2011**, 13, 5294; (c) Fabbri, L.; Marcotte, N.; Stomeo, F.; Taglietti, A. *Angew. Chem., Int. Ed.* **2002**, 41, 3811.
- (a) Valeur, B.; Leray, I. *Inorg. Chim. Acta* **2007**, 360, 765; (b) Kim, S. H.; Kim, H. J.; Yoon, J.; Kim, J. S. In *Calixarenes in the Nanoworld*; Vicens, J., Harrowfield, J., Eds.; Springer: Dordrecht, The Netherlands, 2007, Chapter 15; (c) Valeur, B.; Bourson, J.; Pouget, J.; Czarnik, A. W. *Fluorescent Chemosensors for Ion and Molecule Recognition*. ACS Symposium Series 538; American Chemical Society: Washington, DC, 1993; (d) Sharp, S. L.; Warmack, R. J.; Goudonnet, J. P.; Lee, I.; Ferrell, T. L. *Acc. Chem. Res.* **1993**, 26, 377.
- Yoon, S.; Albert, A. E.; Wong, A. P.; Chang, C. J. *J. Am. Chem. Soc.* **2005**, 127, 16030.
- (a) Shahid, M.; Srivastava, P.; Misra, A. *New J. Chem.* **2011**, 35, 1690; (b) Misra, A.; Shahid, M.; Srivastava, P. *Sens. Actuators, B* **2012**, 169, 327.
- Benesi, H. A.; Hildebrand, J. H. *J. Am. Chem. Soc.* **1949**, 71, 2703.
- Lakowicz, J. R. *Principles of Fluorescence Spectroscopy*, 2nd ed.; Kluwer Academic/Plenum: New York, NY, 1999.
- Frisch, M. J.; Trucks, G. W.; Schlegel, H. B. *GAUSSIAN 03, Revision E.01*; Gaussian: Wallingford, CT, 2007.
- (a) de Silva, A. P.; Gunarantane, H. Q. N.; Gunnlaugsson, T.; Huxley, A. J. M.; McCoy, C. P.; Rademacher, J. T.; Rice, T. E. *Chem. Rev.* **1997**, 97, 1515; (b) Martinez-Manez, R.; Sancenon, F. *Chem. Rev.* **2003**, 103, 4419.
- Sluys, W. G. V. D. *J. Chem. Educ.* **2001**, 78, 111.
- (a) Sun, S.-S.; Lees, A. J. *Chem. Commun.* **2000**, 1687; (b) Anzenbacher, P.; Tyson, D. S., Jr.; Jursikova, K.; Castellano, F. N. *J. Am. Chem. Soc.* **2002**, 124, 6232; (c) Gimeno, N.; Li, X.; Durrant, J. R.; Vilar, R. *Chem.—Eur. J.* **2008**, 14, 3006; (d) Lee, K.-S.; Lee, J. T.; Hong, J.-I.; Kim, H.-J. *Chem. Lett.* **2007**, 36, 816.